Structural Engineering and Mechanics, *Vol. 66, No. 5 (2018) 569-582*
DOI: https://doi.org/10.12989/sem.2018.66.5.569

Experimental and numerical simulating of the crack separation on the tensile strength of concrete

Vahab Sarfarazi[1], Hadi Haeri*[2], Alireza Bagher Shemirani[3], Zheming Zhu[4] and Mohammad Fatehi Marji[5]

[1]Department of Mining Engineering, Hamedan University of Technology, Hamedan, Iran
[2]Young Researchers and Elite Club, Bafgh Branch, Islamic Azad University, Bafgh, Iran
[3]Department of Civil Engineering, Sadra Institute of Higher Education, Tehran, Iran
[4]College of Architecture and Environment, Sichuan University, Chengdu 610065, China
[5]Mine Exploitation Engineering Department, Faculty of Mining and Metallurgy, Institution of Engineering, Yazd University, Yazd, Iran

(Received January 30, 2018, Revised March 8, 2018, Accepted March 9, 2018)

Abstract. Effects of crack separation, bridge area, on the tensile behaviour of concrete are studied experimentally and numerically through the Brazilian tensile test. The physical data obtained from the Brazilian tests are used to calibrate the two-dimensional particle flow code based on discrete element method (DEM). Then some specially designed Brazilian disc specimens containing two parallel cracks are used to perform the physical tests in the laboratory and numerically simulated to make the suitable numerical models to be tested. The experimental and numerical results of the Brazilian disc specimens are compared to conclude the validity and applicability of these models used in this research. Validation of the simulated models can be easily checked with the results of Brazilian tests performed on non-persistent cracked physical models. The Brazilian discs used in this work have a diameter of 54 mm and contain two parallel centred cracks (90° to the horizontal) loaded indirectly under the compressive line loading. The lengths of cracks are considered as; 10 mm, 20 mm, 30 mm and 40 mm, respectively. The visually observed failure process gained through numerical Brazilian tests are found to be very similar to those obtained through the experimental tests. The fracture patterns demonstrated by DEM simulations are mostly affected by the crack separation but the tensile strength of bridge area is related to the fracture pattern and failure mechanism of the testing samples. It has also been shown that when the crack lengths are less than 30 mm, the tensile cracks may initiate from the cracks tips and propagate parallel to loading direction till coalesce with the other cracks tips while when the cracks lengths are more than 30 mm, these tensile cracks may propagate through the intact concrete itself rather than that of the bridge area.

Keywords: experimental tests; discrete element method; Brazilian discs; non-persistent cracks; crack separation

1. Introduction

The heterogeneous solids containing cracks can be regarded as rocks, concrete and rock-like materials. These materials are mostly brittle and may behave elastically under different loading conditions. As far as the cracks are concerned, they may initiate from the defects, propagate and coalesce with the neighbouring cracks to form bigger cracks or discontinuities. This process may decrease the rocks and concrete strength and cause the brittle failure of solids with one or more cracks. Fracture mechanics usually deals with the brittle failure of the rocks and concrete specimens with or without discontinuities. Some extensive research has been performed on the important areas of cracked concrete behaviours under compression. Experimental studies have been accomplished on the rock like materials (Reyes and Einstein 1991, Shen and Stephansson 1993, Shen *et al.* 1995, Bobet and Einsein 1998, Wong and Chau 1998, Scavia and Castelli 1998, Mughieda and Alzoubi 2004) and in situ rocks (Ingraffea and Heuze 1980, Petit and Barquins 1988, Jiefan *et al.* 1990). These brittle materials mainly contain one or two pre-existing inclined cracks passing through the sample thickness and loaded uni-axially under compression. These experimental works illustrate a common fracture pattern which involves wing and secondary cracks in the failed rock samples. Bobet (2000) in his experimental work show that these fracturing patterns may occur through the initiation of the wing cracks at the pre-existing crack tips which may follow by their propagation, in a curvilinear path, under increasing the compressive load with a tendency to align in the direction of the major principal stress.

The Brazilian disc tests are among the most versatile tests for studying the fracture mechanism of rocks and rock-like specimens containing central pre-existing crack (Awaji and Sato 1978, Sanchez 1979, Atkinson 1982, Shettyetal 1986, Krishnan *et al.* 1998, Khan and Al-Shayea 2000, Al-Shayea *et al.* 2000, Al-Shayea 2005, Wang 2010, Wang *et al.* 2011, 2012, Ghazvinian *et al.* 2013, Bahaaddini *et al.* 2013, Yang 2015, Wei *et al.* 2015, Haeri *et al.* 2015, Li *et al.* 2015, Li *et al.* 2016, Li *et al.* 2016, Haeri *et al.* 2016, Shaowei *et al.* 2016, Wang *et al.* 2017, Shemirani *et al.* 2016, Shemirani *et al.* 2017, Sarfarazi *et al.* 2017a, b, c, Shemirani *et al.* 2018). Some experimental and numerical

*Corresponding author, Ph.D.
E-mail: h.haeri@bafgh-iau.ac.ir or haerihadi@gmail.com

http://www.techno-press.com/journals/sem&subpage=7
ISSN: 1225-4568 (Print), 1598-6217 (Online)

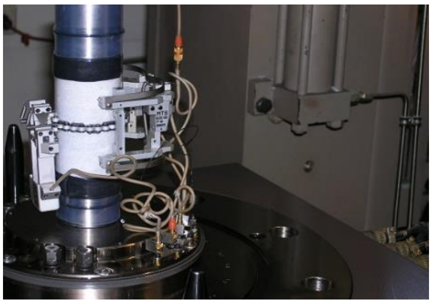

(a)

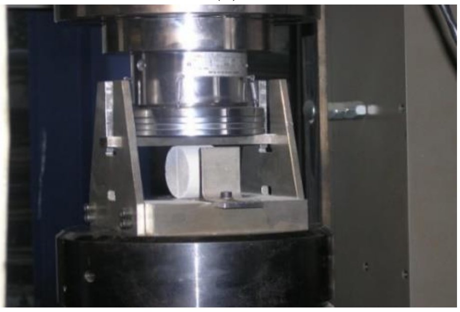

(b)

Fig. 1(a) Uniaxial compression test, (b) Brazilian tensile test

Table 1 Specification of grain size, mixture ratio and their mechanical properties

Material mixture	Grain size (mm)	Mixture ratio	Density (kg/m3)	Uniaxialstrength (MPa)	Tensile strength (MPa)
Cement/grain/water	0.3-2.5	1/0.5/1	2100	43.7	4.1
Cement/grain/water	0.05-0.5	0.75/0.5/1	1660	29.2	2.6
Cement/grain/water	0.005-0.2	0.5/1/1	1900	53.3	4.6
gypsum/water	0.001-0.01	0.5/1/1	1900	53.3	4.6

works carried out by Ghazvinian *et al.* (2013) to detect the cracks initiation and propagation in CSCBD specimens. Wong (2002) proposed the Rock Failure Process Analysis (RFPA2D) code, Park (2008) introduced the FROCK code, Lee (2014) and Manouchehrian *et al*. (2014) used the 2D Particle Flow Code (PFCD) to study the fracture mechanics of brittle rocks.

A few centre cracks have been studied in most of the previous researches using the Brazilian disc specimens because of the difficulties in producing these specimens in the laboratory so that they contain multiple cracks. However, the cracks initiation stresses, the failure stresses, the cracks propagation and cracks coalescence have been investigated experimentally and numerically by simulating the Brazilian discs of concrete samples containing multiple cracks in their central parts. These numerical results are validated by the experimental studies and also with the corresponding results cited by the other numerical results already exist in the concrete fracture mechanics literature. The two-dimensional explicit discrete element method in form of a particle flow code is used in this paper to analyse the fracturing process of the Brazilian disc concrete specimens. These validated numerical models may be useful for further studying of the mechanical behaviour of the pre-existing cracks in the discontinuous concrete.

(a)

(b)

(c)

(d)

Fig. 2 The fracturing patterns in the modelled samples with tensile strengths of (a) 0.9 MPa, (b) 1.6 MPa, (c) 2.1 MPa and (d) 2.5 MPa

2. Experimental set up of the Brazilian discs with parallel joints

The Brazilian disc type specimens containing joints (cracks) are being tested under diametrical loading. The experimental set up of these testing specimens are explained in this section.

2.1 Modelling material and its physical properties

The tensile behaviour of bridge areas is being studied by preparing and testing the Brazilian type of specimens specially prepared from a mixture of three concrete types. These specimens are prepared by mixing cement, rock chips (sands or grains), gypsum and water. The material mixtures, their grain sizes and their mixture ratios for four different mixtures are given in Table 1. The uniaxial compression tests and Brazilian tensile tests are accomplished to

(a)

(b)

(c)

Fig. 3 The mould used for the casting of the jointed specimens; (a) mould with internal sheet, (b) mould with material mixture, (c) front and side views of the mould

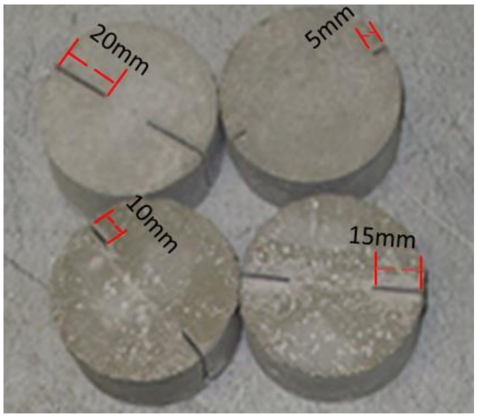

(a)

(b)

(c)

(d)

Fig. 4 The non-persistent joints with tensile strengths of; (a) 0.9 MPa, (b) 1.6 MPa, (c) 2.1 MPa and (d) 2.5 MPa

determine the mechanical properties of these four different mixtures. The Brazilian type cylindrical specimens each having a diameter of 56 mm and a length of 112 mm are prepared with these four types of mixtures to measure the uniaxial compressive strength (UCS) of the modelled material samples. The Brazilian discs with 54 mm in diameter and 25 mm in thickness are also being used to determine the indirect Brazilian tensile strength (BTS) of these modelled materials. These two testing procedures (UTS and BTS) are complied with the ASTM D2938-86 and ASTM C496-71, codes respectively. The testing set up of these experiments are shown in Fig. 1(a) and Fig. 1(b).

Table 1 shows the mechanical properties of the four mixtures used in this research.

Fig. 2 shows the indirect tensile failure process occurred in the four specific Brazilian test specimens of the four types of modelled materials samples used in this study.

2.2 Preparation and testing of concrete modelled samples with non-persistent joints

The modelled samples are prepared by mixing, casting and curing of specimens and are carefully controlled to obtain some reproducible specimens with prescribed properties. A special blender is used to mix the material constituents of the specimens and a special mould is also used to cast these material in form of concrete discs'

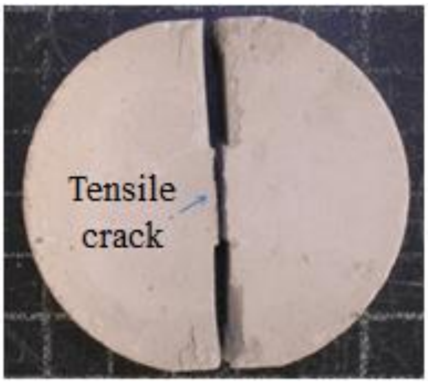

(a)

(b)

(c)

(d)

Fig. 5 The fracture patterns and failure modes for the Brazilian tests specimens with the joint ratios (JC) of; (a) 0.18, (b) 0.37, (c) 0.55 and (d) 0.74; the samples tensile strength is 0.9 MPa

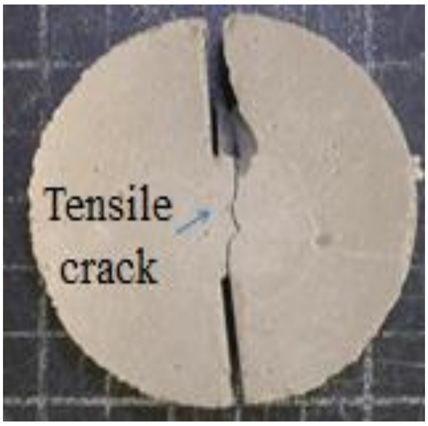

(a)

(b)

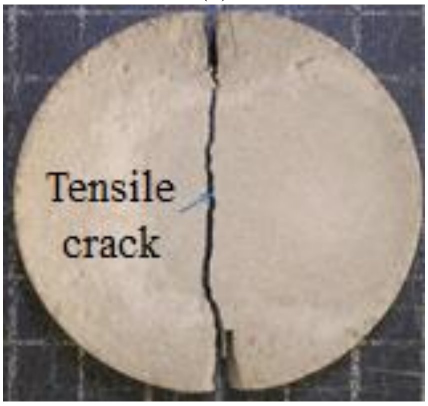

(c)

(d)

Fig. 6 The fracture patterns in the Brazilian tests with the joint ratios of; (a) 0.18, (b) 0.37, (c) 0.55 and (d) 0.74; the tensile strength of the intact samples is 1.6 MPa samples (Fig. 3(a)). Two semi-cylinders with a diameter of 90 mm and thickness 27 mm are bolted to each other with an elastic band to form this sample casting mould (Fig. 3(b)). Then, two pairs of thin blades each having a thickness of 1 mm and a length of 100 mm are used to create the non-persistent joints in the samples (Fig. 3(a)). However, the lengths of these blades changes as 5, 10, 15, and 20 mm (Fig. 3(a)) for different modelled samples. These blades are greased and inserted through the mould before the mixture pouring operation (Fig. 3(c)). It takes 30 minutes for each sample to be casted in the mould and then it is removed and the internal part of the sample is pulled out from the specimen. The blade removal is taking place easily because of the grease already attached to the blades surfaces before sample casing operation. The joints (parallel cracks) in the specimens are produced by the internal blades through the entire thickness and at right angles to the front and back sides of these samples so that these joints are open (joint aperture) about 1 mm. The grease is covered the internal blades so that their removal may not produce any damage to the specimens. These casted specimens are kept at room temperature (20 ± 2ºC) for 10 days in the laboratory. It should be noted that the mixing, casting, curing and testing operations of the specimens should be carefully accomplished such that the acceptable testing results can be experimentally gained.

As shown in Fig. 4, four specimens with different joint length i.e., 1, 2, 3 and 4 cm are prepared from each mixture type such that the ratio of joint lengths to the sample diameter (JC) are 0.18, 0.37, 0.55 and 0.74, respectively. The sample testing can be accomplished by a servo-controlled MTS apparatus in a mechanics laboratory. The displacement rate for all testing samples is kept as 0.01 mm/s. A data acquisition system is being used to measure the normal loads and displacements during the testing.

2.3 Effects of joint ratio on the failure pattern

The effects of joint ratio on the fracturing pattern and failure process of the four testing models with different tensile strengths are shown in Figs 5-8, respectively. Formation of new fractures initiating from the joints tips due to the shearing process of a discontinuous joint eventually may break away the intact materials within the bridge areas and lead to a relatively big through-going discontinuity. These testing observations of the fracturing surfaces through the bridge areas illustrate the fracturing patterns and failure mechanism of the modelled Brazilian samples as shown in Fig. 5. The tensile cracks initiate from the joint tips for the joint ratios, JC=0.18. 0.37 and 0.55 as shown in Figs. 5(a), 5(b) and 5(c), respectively. These tensile cracks propagate vertically till coalesce with each other or with the other joint tip. It is observed that the fracture surface at the bridge area is due to tensile mode of failure because its surface is varnished with no crushed materials. As shown in Fig. 5(d) for the joint ratio of JC=0.74, at the time of failure of the samples, these tensile cracks may start their initiation from the sample's centre and then propagate vertically toward the sample edges (in the direction of compressive loading) till they meet the upper and lower parts of the sample.

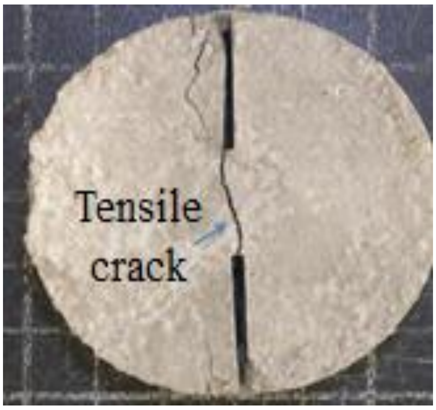

(a)

(b)

(c)

(d)

Fig. 7 The fracturing patterns at the failure stage in the Brazilian test samples with joint ratios of; (a) 0.18, (b) 0.37, (c) 0.55 and (d) 0.74; the intact sample's tensile strength is 2.1 MPa

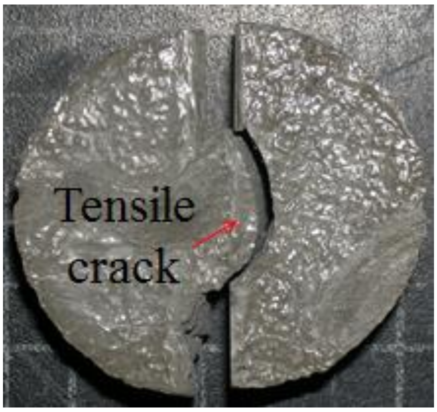

(a)

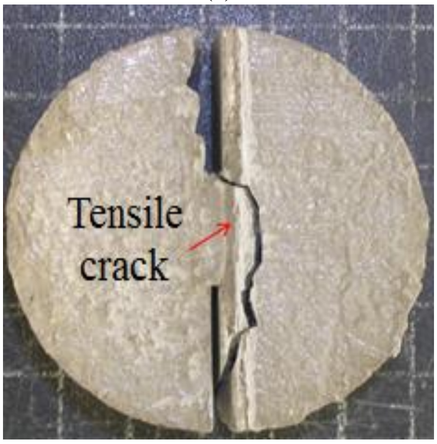

(b)

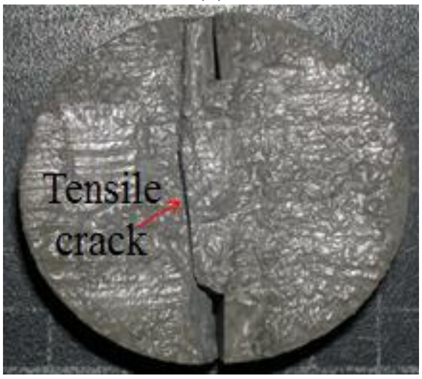

(c)

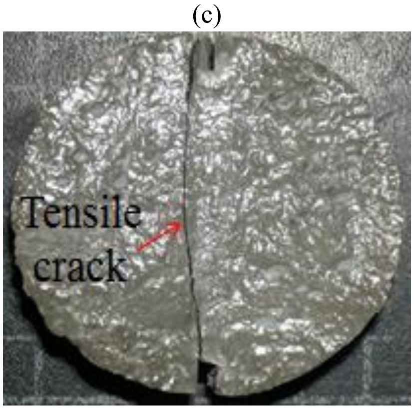

(d)

Fig. 8 The fracture patterns at the failure stage of the Brazilian test samples with joint ratios (JC) of; (a) 0.18, (b) 0.37, (c) 0.55 and (d) 0.74; the intact sample's tensile strength is 2.5 MPa

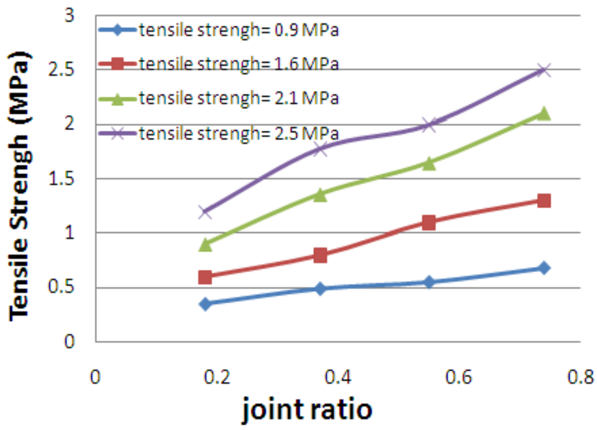

Fig. 9 The variation of the tensile strength of the tested samples versus the joint ratio

The tensile cracks may initiate from the joint tips for the joint ratios, 0.18 and 0.37 as shown in Fig. 6(a) and Fig. 6(b), respectively. These cracks may further propagate vertically till coalesce with the tip of other joint in the modelled sample. The fracture surface at the failure line of the bridge areas show a tensile mode of fracture because its surface is varnished and there are not any crushed materials on it during the failure process of these samples.

As shown in Fig. 6(c) for the joint ratio of 0.55, at the first stage of failure process, the tensile cracks may initiate from the join tip and propagate vertically till coalesce with other joint tip. Then, the secondary tensile cracks may initiate at the sample edges and propagate vertically till coalesce with the previously extended cracks.

Fig. 6(d) shows that the tensile cracks may initiate from the sample’s centre for the joint ratio of 0.74 and then they may propagate vertically toward the sample’s edge till meet the upper and lower sides of the sample.

The Figs. 7(a), 7(b), 7(c), and 7(d) show that the tensile cracks initiate from the joint tips and propagate vertically till coalesce with the other joint tip for the joint ratios 0.18, 0.37, 0.55 and 0.74, respectively. For all these cases, the fracture surfaces at the failure stage of the bridge areas in the modelled samples are of tensile modes because these surfaces are varnished with no crushed materials on them.

Fig. 8(a) shows that the tensile crack may initiates from the joint tip and propagates vertically till coalesce with the other joint tip for a joint ratio of 0.18. The fracturing surface at the bridge area of the modelled samples is due to a tensile mode of failure because this surface is varnished and no crushed materials are present on it.

The first tensile cracks may initiate for the joint ratio of 0.37 as shown in Fig. 8(b). These cracks initiates from the tip of the upper joint and propagate vertically till meet the lower joint's wall.

For the joint ratio of 0.55, the tensile cracks may initiate from the lower joint tip and propagates vertically toward the sample’s edge till meet the upper edge of the sample (Fig. 8(c)). The tensile cracks may start their initiation from the sample’s centre (Fig. 8(d)) for the joint ratio of 0.74 and then may propagate vertically toward the sample’s edge till meet the upper and lower parts of the modelled sample.

2.4 Effects of joint ratio on the tensile strength of the modelled samples

Variation of the tensile strengths versus the joint ratios for these four different concrete samples are shown graphically in Fig. 9. These results illustrate that the tensile strength is increased as the joint ratio is increased for modelled samples.

3. Discrete element modelling of the experimentally tested samples

The explicit discrete element modelling technics are now widely used to simulate the concrete behaviours in recent years. This method is relatively simple because it's formulations are explicit and does not require a complex implicit formulations of the constitutive models (Ghazvinian *et al.* 2013).

Several researchers worked on the discrete element modelling of rocks, concrete and rock like materials. The nonlinear failure behaviour of the intact materials may be difficult to be accurately simulated by the ordinary discrete element method utilizing the circular particles (Diederich, 2000). On the other hand, the clump bonded particle models suggested by Cho *et al.* (2007) may be used to overcome the shortcomings identified by Diederich (2000). However, the clumped bonded particle model was developed for the commercially available discrete element code, such as the two dimensional particle flow code (PFC2D). An assemblage of the rigid particles bonded together with cohesive and frictional bonds may be used in a particle flow code where the circular disc type elements can be confined by using the planar walls in a two dimensional discrete element code. The cracked concrete specimen have been extensively modelled by the two dimensional universal distinct element code (UDEC) developed by Cundall (2000). However, in PFC codes the forces and motions of individual particles are being modelled within an assembly of rigid particles bonded to each other at the contact points so that each particle can move independently from the other particles but interact only at the contact points. Although the particles are rigid but they can overlap at the contact s when the modelled sample is under compression. In the particle flow code. the particles themselves are rigid and never deform because they can only undergo rigid body motion. The shear and tensile strengths at these bonded particles are at each contact (bonded) point. However, the macro strength of the modelled samples and their mechanism of failure and fracturing are highly influenced by the assigned bonding strengths during loading. The frictional coefficient of the bonded particles is specified for each bonding model to activate the frictional force during loading of the samples as long as the bonded particles stay in contact. As the applied normal stress exceeds the specified normal bonding strength of the bonded particles the tensile cracks may occur within the samples. On the other hand, the shear cracks may be produced due to the particles rotation or their shearing within the samples as the applied shear stress exceeds the specified shear bond strength of the bonded particles. After each bonding breakage, the tensile strength at the contact point immediately drops to zero and the shear strength of the

Table 2 Micro properties of the concrete samples in the numerical models

Parameter	Value	Parameter	Value
Type of particle	Disc	Parallel bond radius multiplier	1
Density	3000	Young modulus of parallel bond (GPa)	40
Minimum radius	0.27	Parallel bond stiffness ratio	1.7
Size ratio	1.56	Particle friction coefficient	0.4
Porosity ratio	0.08	Parallel bond normal strength, mean (MPa)	5
Damping coefficient	0.7	Parallel bond normal strength, SD (MPa)	2
Contact young modulus (GPa)	40	Parallel bond shear strength, mean (MPa)	5
Stiffness ratio	1.7	Parallel bond shear strength, SD (MPa)	2

Table 3 Micro properties of the numerical models with tensile strength of 4.6 MPa

Property	Value	Property	Value
Type of particle	disc	Parallel bond radius muliplier	1.4
Densiy (kg/m3)	3000	Youngs modulus of parallel bond (GPa)	1.7
Minimum radius (mm)	0.27	Parallel bond stifness ratio	3
Size ratio	1.56	Particle friction coefficien	0.5
Porosity ratio	0.05	Parallel normal strength, mean (MPa)	11
Local damping coefficient	0.7	Parallel normal strength, std. dev (MPa)	2
Contact young modulus (GPa)	12	Parallel shear strength, mean (MPa)	11
Stiffness ratio (kn/ks)	1.7	Parallel shear strength, std. dev (MPa)	2

Table 4 Micro properties of the numerical models with tensile strength of 2.6 MPa

Property	Value	Property	Value
Type of particle	disc	Parallel bond radius muliplier	1.4
Densiy (kg/m3)	2200	Youngs modulus of parallel bond (GPa)	1.7
Minimum radius (mm)	0.27	Parallel bond stifness ratio	3
Size ratio	1.56	Particle friction coefficien	0.5
Porosity ratio	0.05	Parallel normal strength, mean (MPa)	18
Local damping coefficient	0.7	Parallel normal strength, std. dev (MPa)	5
Contact young modulus (GPa)	12	Parallel shear strength, mean (MPa)	18
Stiffness ratio (kn/ks)	1.7	Parallel shear strength, std. dev (MPa)	5

Table 5 Micro properties of the numerical model with tensile strength of 4.1 MPa

Property	Value	Property	Value
Type of particle	disc	Parallel bond radius muliplier	1.4
Densiy (kg/m3)	2600	Youngs modulus of parallel bond (GPa)	1.7
Minimum radius (mm)	0.27	Parallel bond stifness ratio	3
Size ratio	1.56	Particle friction coefficien	0.5
Porosity ratio	0.05	Parallel normal strength, mean (MPa)	14
Local damping coefficient	0.7	Parallel normal strength, std. dev (MPa)	5
Contact young modulus (GPa)	12	Parallel shear strength, mean (MPa)	14
Stiffness ratio (kn/ks)	1.7	Parallel shear strength, std. dev (MPa)	5

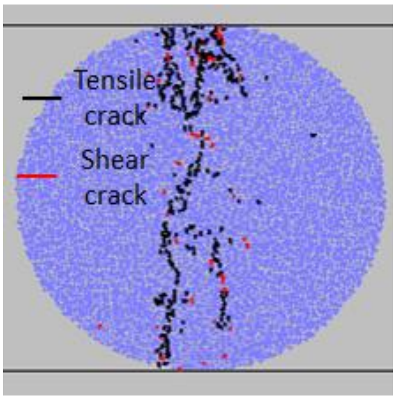

(a)

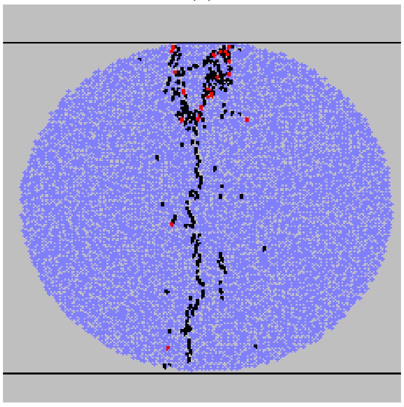

(b)

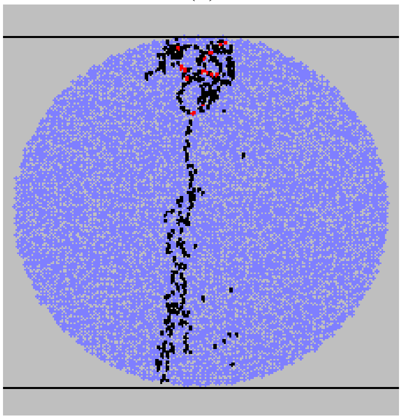

(c)

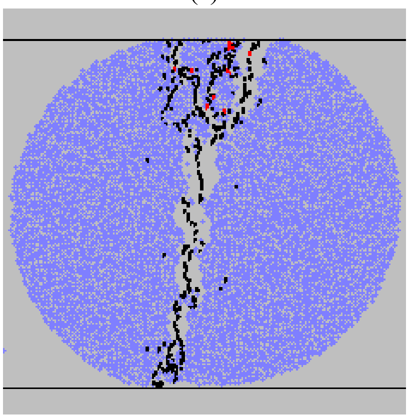

(d)

Fig. 10 Fracture patterns in the numerical models with the tensile strength of (a) 1MPa, (b) 1.8 MPa, (c) 2.3 MPa and (d) 2.7 MPa

Table 6 Brazilian tensile strength of the physical and numerical samples

Mechanical properties	Model I	Model II	Model III	Model IV
Physical tensile strength (MPa)	0.9	1.6	2.1	2.5
Numerical tensile strength (MPa)	1	1.8	2.3	2.7

bonding particles decreases to its residual friction (Ghazvinian *et al.* 2013). The specified coefficient of friction and the induced normal contact force governs the residual shear strength of the sample. The localized progressive failure of the sample may occur after each bonding breakages process because the stresses are redistributed within the sample (Lambert and Coll 2013).

It should be noted that for all these microscopic behaviours, the particle flow code needs no plastic flow rule (theory of plasticity) to govern the samples behaviour but only the basic micro-parameters are describing the contact and bonding stiffness. The bonding strength and the contact friction are specified by the micro-parameters which provide the macro-scale behaviour of the modelled material. The particle flow code uses an explicit finite difference scheme to numerically solve the equations of force and motion therefore, the initiation and propagation of bonding breakage process within the material can be tracked and the failure process at each contact point can be tackled and the dominant mode of failure (tensile or shear modes) can be easily determined (Sarfarazi *et al.* 2014).

3.1 Preparing and calibrating the numerical models

The Brazilian tensile strength (BTS) of the specimens are used to calibrate the numerically simulated samples by particle flow code. Generally, four steps are involved in the numerical modelling of the bonded particles by a standard particle flow code: (a) generation and packing of the particles, (b) assuming and installing an isotropic stress condition, (c) eliminating the floating particles, and (d) installing the particle bonding condition.

Tables 2, 3, 4, and 5 give the adopted micro-properties of the modelled samples and the standard calibration procedures for the numerical simulation of the particles assembly in the testing materials (Potyondy and Cundall 2003). However, the numerically simulated Brazilian discs considered in the numerical tests is also of 54 mm in diameter and 5,615 particles are used to model each testing sample. A displacement control modelling technique is used by applying a low speed of 0.016 m/s to crush the lateral walls of the disc samples.

The fracture patterns of the numerically simulated samples with four different tensile strengths are shown in Fig. 10(a) to Fig. 10(d), respectively. Comparing these figures with their corresponding experimentally gained Figs. 2(a) to 2(d) it can be easily observed that the fracture patterns and the failure process of the modelled samples are well matching.

The numerical tensile strength and a comparison of its experimental measurements were presented in Table 6. This table shows a good accordance between numerical and experimental results.

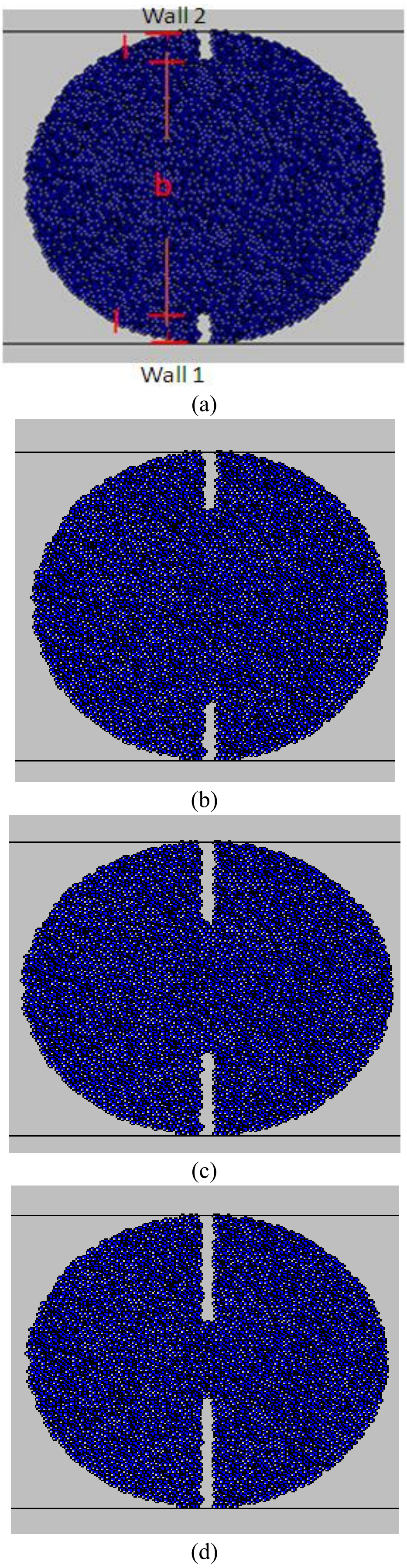

Fig. 11 Numerical non-persistent joint with joint length of; (a) 10 cm, (b) 20 cm, (c) 30 cm and (d) 40 cm

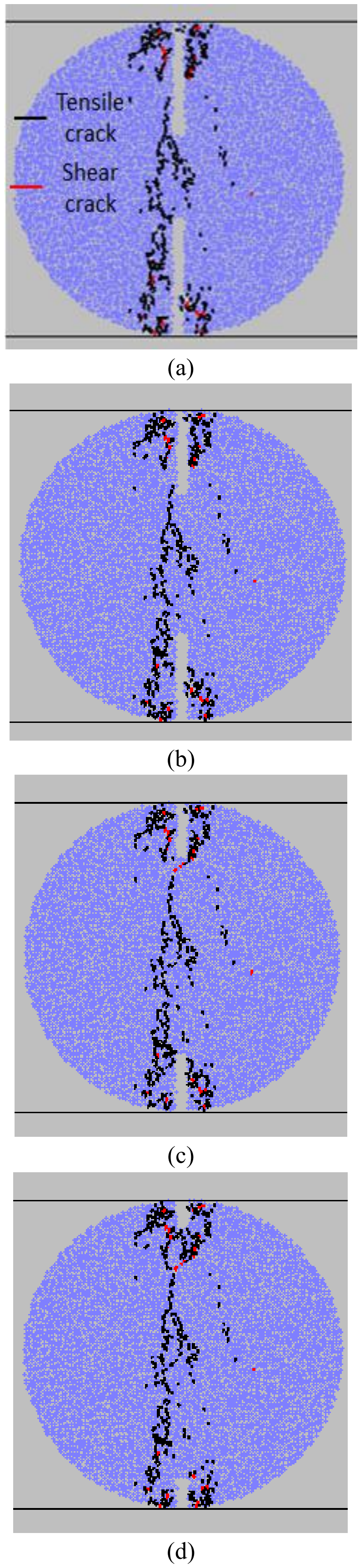

Fig. 12 The fracture patterns obtained numerically in the Brazilian tests with joint ratio (JR) of; (a) 0.18, (b) 0.37, (c) 0.55 and (d) 0.74; the tensile strength of the modelled sample is 1 MPa

3.2 Preparing the numerical models of the tested samples

The Brazilian tensile strength tests are to be simulated numerically by using the circular models with the calibrated micro-parameters already given in Tables 2 to 5 as shown in Figs. 11(a) to 11(d). The modelled specimen is of 54 mm in diameter with a minimum radius of 27 mm. In these numerical analyses, a total of 6543 discs are being used to simulate the Brazilian specimen. The modelled samples of the Brazilian disc type shown in Figs. 11 contain two edge cracks to represent the non-persistent cracks in the real case of a typical concrete type. These modelled cracks are of equal lengths in each model but may be of different lengths in various modelled samples which are considered as 10 mm, 20 mm, 30 mm and 40 mm, respectively. The corresponding numerically and experimentally modelled samples are of equal spacing (b) in between the notches (edge cracks tips) which are taken as 44 mm, 34 mm, 24 mm and 14 mm, respectively. The joint ratio (JR) i.e., the ratio of the joint length to the modelled samples diameter and the joint's opening (joint's aperture) in all of the corresponding numerical model and experimental samples is taken to be similar where the joint's opening is assumed to be 2 mm. The lateral walls of the models are moved toward each other to crush the sample with a low speed of 0.016 m/s. Fig. 11(a) shows the reaction forces on the wall No.1 which produce the tensile forces causing the sample's failure.

4. Effects of joint ratio on the fracturing patterns of the modelled samples

The effects of joint ratio on the fracture pattern of the four types of numerically modelled samples with different tensile strengths are explained in this section.

4.1 Modelled samples with a tensile strength of 1 MPa

The tensile cracks initiating from the joint tips and propagates vertically till coalesce with the other joint tips when the joint ratios (JRs) are 0.18, 0.37, 0.55, 0.74 as shown in Fig. 12(a), (b), (c) and (d), respectively. As it can be observed the tensile strength is too low therefore several tensile bands are developed in the modelled sample. In these figures the black and red lines represent the tensile and shear cracks, respectively.

4.2 Modelled samples with a tensile strength of 1.8 MPa

The tensile cracks initiating from the joint tip and propagates vertically till coalesce with the other joint tip for a joint ratio of 0.18 (Fig. 13(a)) but for the joint ratios 0.37, 0.55 and 0.74 (Fig. 13(b), (c) and (d), respectively), the two broken wedges formed from the top and bottom of the model and then one tensile fracture is developed between these wedges.

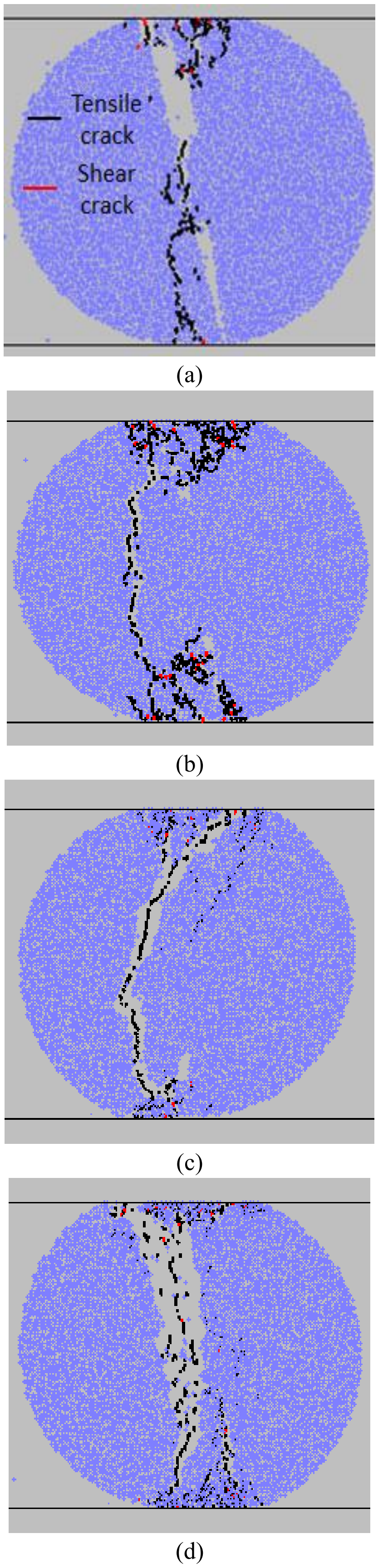

Fig. 13 The fracture patterns numerically obtained in the Brazilian test samples with a joint ratio of; (a) 0.18, (b) 0.37, (c) 0.55 and (d) 0.74; respectively, the tensile strength of the modelled sample is 1.8 MPa

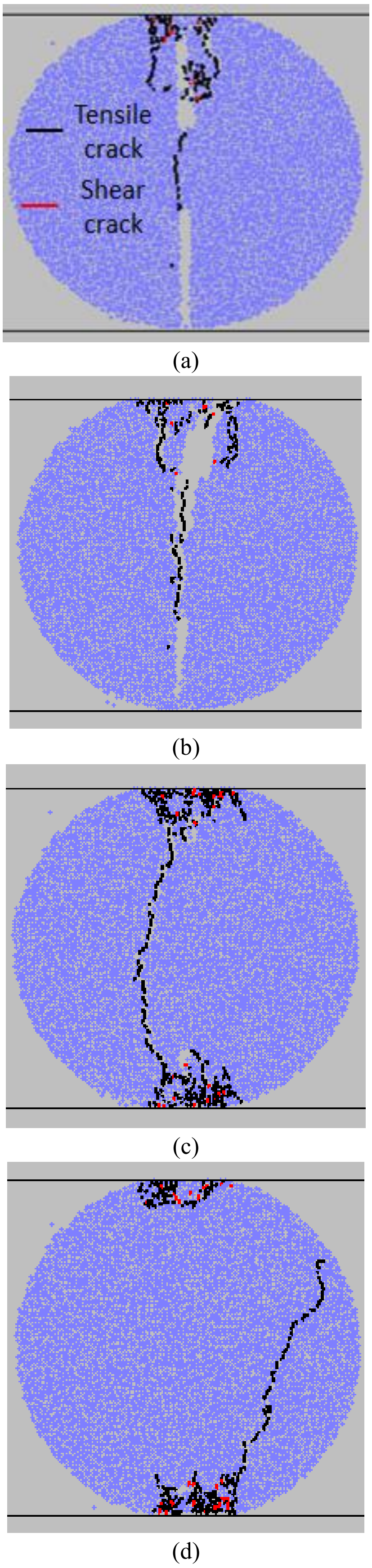

Fig. 14 The fracture patterns obtained numerically in the Brazilian test samples with joint ratios of; (a) 0.18, (b) 0.37, (c) 0.55 and (d) 0.74, respectively; the tensile strength of the sample is 2.3 MPa

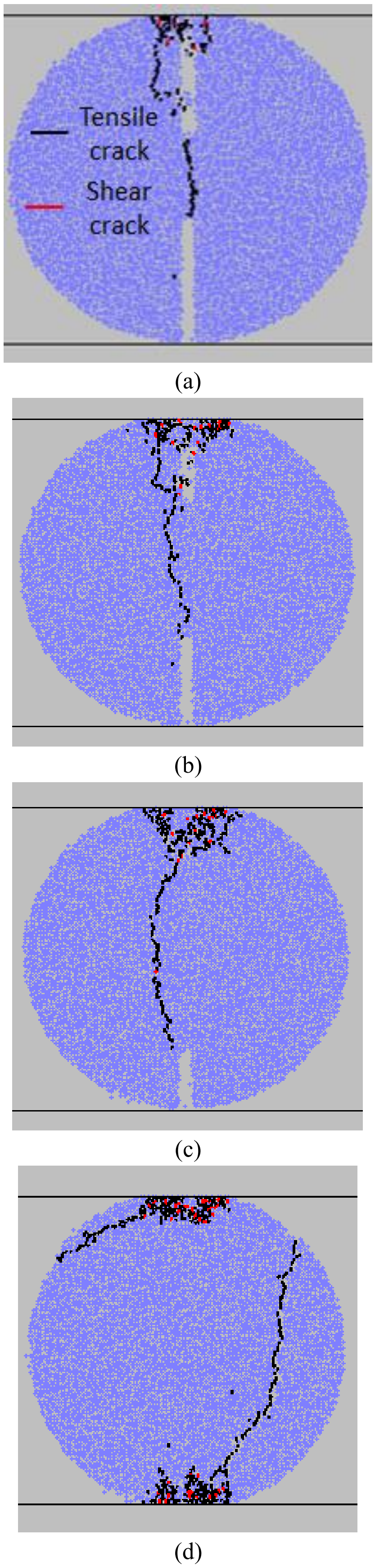

Fig. 15 The fracture patterns of the modelled Brazilian testing samples obtained numerically for the joint ratios of; (a) 0.18, (b) 0.37, (c) 0.55 and (d) 0.74, respectively; the sample's tensile strength is 2.7 MPa

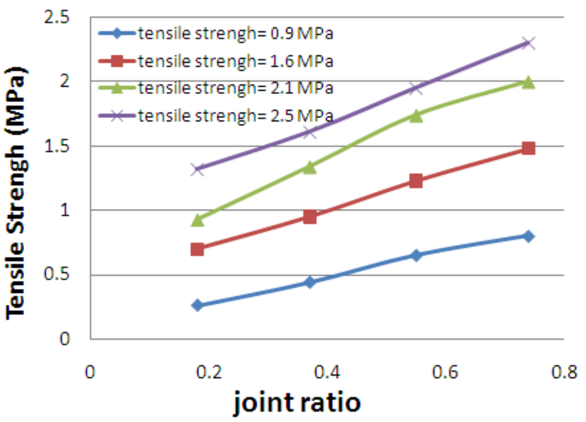

Fig. 16 Variation of the tensile strength versus the joint ratio in the modelled samples

4.3 Modelled samples with a tensile strength of 2.3 MPa

In this case, the tensile strength of the modelled samples with the joint ratios of 0.18 and 0.37 (Fig. 14(a) and (b)) initiating from the joint tip and propagates vertically till coalesce with the other joint tip. As shown in Fig. 14(c), for the samples with joint ratio of 0.55, the two broken wedges are formed from the top and bottom of the model and then one tensile fracture may develop between these wedges but for the samples with a joint ratio of 0.74 (Fig. 14(d)), the tensile cracks initiates at the edge of the sample and propagates diagonally till meet the two sides of the model.

4.4 Modelled samples with a tensile strength of 2.7 MPa

As shown in Fig. 15(a) and Fig. 15(b) for the joint ratios of 0.18, 0.37, respectively, the tensile crack may initiate from the join tip and propagates vertically till coalesce with other joint tip. For the case of jointing ratio of 0.55 (Fig. 15(c)) in the modelled sample, only one separated wedge may be formed at the top section of this model and then one tensile fracture may start its initiation from the lower joint tip and propagates vertically till coalesce with this broken wedge. However, Fig. 15(d) shows that when the joint ratio of the modelled sample is 0.74, the tensile crack may start its initiation from the edge of the sample and propagate diagonally till coalesce with both sides of the model.

5. Effects of the joint ratio on the tensile strength of the modelled samples

The variation of the tensile strength versus the joint ratio for the four different modelled samples with different tensile strengths are shown graphically in Fig. 16. As shown in this figure, the tensile strength of all modelled samples increases as the joint ratio is increased. Therefore, comparing Fig. 16 with its experimental counterpart (already shown in Fig. 9), it can be easily concluded that nearly the same trend of tensile strength is stablished in between the numerical simulation and the experimental tests.

6. Conclusions

The tensile behaviour and fracturing process of the Brazilian disc samples containing non-persistent joints are investigating experimentally and numerically in the present research work. These experimental tests and numerical simulations of the modelled samples with four different tensile strengths and four jointing ratios are carried out simultaneously to provide a thorough understanding of the effects of non-persistent joint behaviours on the tensile strength and failure behaviour of the cracked concrete. In this research, the experimental tensile tests of the Brazilian discs are performed using four different mixtures having different tensile strengths. The modelled sample's diameter is chosen as 54 mm and the joint lengths are assumed to be 10 cm, 20 cm, 30 cm and 40 cm, respectively. The numerical simulations of the same testing samples are also performed to be able to compare the estimated numerical results with their corresponding experimentally measured values. However, the failure stress, cracks propagation mechanism and the cracks coalescence through the modelled samples and within the bridge areas have been studied. Some of the most important conclusions may be categorized as:

- For the joint ratios of 0.4, 0.6 and 0.7, the tensile crack may start its initiation from the join tip and propagates vertically till coalesce with other joint tip.
- At the same time, it may be concluded that the fracture surface at the bridge area is tensile because this surface is varnished and no crushed materials are present.
- For a higher joint ratio (i.e., 0.85), the edge cracks grow through the modelled samples and the bridge area is unbroken.
- The tensile strengths of the all experimentally tested samples increases with increasing the joint ratio.
- All of the above-mentioned results can also be concluded from the simultaneous numerical simulation of the modelled samples by comparing these results with their corresponding experimental counterparts.
- These comparisons show that there is a very good agreement in between the experimental and numerical results.
- It may be concluded that the discrete element modelling technics can be successfully used for the investigations on the failure and fracture analyses of the cracked concrete specimen.

References

Al-Shayea, N.A. (2005), “Crack propagation trajectories for rocks under mixed mo de I-II fracture”, *Eng. Geol.*, **81**(1), 84-97.

Al-Shayea, N.A., Khan, K. and Abduljauwad, S.N. (2000), “Effects of confining pressure and temperature on mixed-mode (I-II) fracture toughness of a limes tone roc k formation”, *Int. J. Rock Mech. Rock Eng.*, **37**(4), 629-643.

Atkinson, C., Smelser, R.E. and Sanchez, J. (1982), “Combined mode fracture via the cracked Brazilian disk”, *Int. J. Fract.*, **18**(4), 279-291.

Awaji, H. and Sato, S. (1978), "Combined mode fracture toughness measurement by the disk test", *J. Eng. Mater. Technol.*, **100**(2), 175-182.

Ayatollahi, M.R. and Aliha, M.R.M. (2008), "On the use of Brazilian disc specimen for calculating mixed mode I-II fracture toughness of rock materials", *Eng. Fract. Mech.*, **75**(16), 4631-4641.

Ayatollahi, M.R. and Sistaninia, M. (2011), "Mode II fracture study of rocks using Brazilian disk specimens", *Int. J. Rock Mech. Min. Sci.*, **48**(5), 819-826.

Bagher Shemirani, A., Haeri, H., Sarfarazi, V. and Hedayat, A. (2017), "A review paper about experimental investigations on failure behaviour of non-persistent joint", *Geomech. Eng.*, **13**(4), 535-570.

Bagher Shemirani, A., Sarfarazi, V., Haeri, H., Marji, M. and Hosseini, S. (2018), "A discrete element simulation of a punch-through shear to investigate the confining pressure effects on the shear behaviour of concrete cracks", *Comput. Concrete*, **21**(2), 189-197.

Bahaaddini, M., Sharrock, G. and Hebblewhite, B.K. (2013), "Numerical investigation of the effect of joint geometrical parameters on the mechanical properties of a non-persistent jointed rock mass under uniaxial compression", *Comput. Geotech.*, **49**, 206-225.

Bobet, A. (2000), "The initiation of secondary cracks in compression", *Eng. Fract. Mech.*, **66**(2), 187-219.

Bobet, A. and Einstein, H.H. (1998), "Fracture coalescence in rock-type materials under uniaxial and biaxial compression", *Int. J. Rock Mech. Min. Sci.*, **35**(7), 863-888.

Cho, N. (2008), "Discrete element modeling of rock: pre-peak fracturing and dilation", Ph.D. Dissertation, University of Alberta, Canada.

Cho, N., Martin, C.D. and Sego, D.C. (2007), "A clumped particle model for rock", *Int. J. Rock Mech. Min. Sci.*, **44**(7), 997-1010.

Cundall, P.A. (1971), "A computer model for simulating progressive large scale movements in blocky rock systems", *Proceedings of the ISRM Symposium*.

Cundall, P.A. (2000), "A discontinuous future for numerical modelling in geomechanics", *Geotech. Eng.*, **149**(1), 41-47.

Diederichs, M.S. (2000), "Instability of hard rock masses: The role of tensile damage and relaxation", Ph.D. Dissertation, University of Waterloo, Canada.

Ghazvinian, A., Nejati, H.R., Sarfarazi, V. and Hadei, M.R. (2013), "Mixed mode crack propagation in low brittle rock-like materials", *Arab J. Geosci.*, **6**(11), 4435-4444.

Haeri, H. (2015), "Influence of the inclined edge notches on the shear-fracture behavior in edge-notched beam specimens", *Comput. Concrete*, **16**(4), 605-623.

Haeri, H., Khaloo, A. and Marji, M.F. (2015), "Experimental and numerical simulation of the microcrack coalescence mechanism in rock-like materials", *Strength Mater.*, **47**(5), 740-754.

Haeri, H., Sarfarazi, V. and Hedayat, A. (2016), "Suggesting a new testing device for determination of tensile strength of concrete", *Struct. Eng. Mech.*, **60**(6), 939-952.

Hazzard, J.F. and Young, R.P. (2000), "Simulating acoustic emissions in bonded-particle models of rock", *Int. J. Rock Mech. Min. Sci.*, **37**(5), 867-872.

Ingraffea, A.R. and Heuze, F.E. (1980), "Finite element models for rock fracture mechanics", *Int. J. Numer. Anal. Meth. Geomech.*, **4**(1), 25-43.

Itasca Consulting Group (2004), *PFC2D (Particle Flow Code in 2 Dimensions) Version 3.1*.

Jiefan, H., Ganglin, C., Yonghong, Z. and Ren, W. (1990), "An experimental study of the strain field development prior to failure of a marble plate under compression", *Tectonophys.*, **175**(1-3), 269-284.

Khan, K. and Al-Shayea, N.A. (2000), "Effects of specimen geometry and testing method on mixed-mode I-II fracture toughness of a limestone rock from Saudi Arabia", *Rock Mech. Rock Eng.*, **33**(3), 179-206.

Krishnan, G.R., Zhao, X.L., Zaman, M. and Rogiers, J.C. (1998), "Fracture toughness of a soft sandstone", *Int. J. Fract. Mech.*, **35**(6), 195-218.

Lambert, C. and Coll, C. (2013), "Discrete modeling of rock joints with a smooth-joint contact model", *J. Rock Mech. Geotech. Eng.*, **6**(1), 1-12.

Li, J.Y., Zhou, H., Zhu, W. and Li, S. (2016), "Experimental and numerical investigations on the shear behavior of a jointed rock mass", *Geosci. J.*, **20**(3), 371-379.

Li, S., Wang, H., Li, Y., Li, Q., Zhang, B. and Zhu, H. (2016), "A new mini-grating absolute displacement measuring system for static and dynamic geomechanical model tests", *Measure.*, **82**, 421-431.

Li, Y., Zhou, H., Zhu, W., Li, S. and Liu, J., (2015), "Numerical study on crack propagation in brittle jointed rock mass influenced by fracture water pressure", *Mater.*, **8**(6), 3364-3376.

Manouchehrian, A., Sharifzadeh, M., Marji, M.F. and Gholamnejad, J. (2014), "A bonded particle model for analysis of the flaw orientation effect on crack propagation mechanism in brittle materials under compression", *Arch. Civil Mech. Eng.*, **14**(1), 40-52.

Mughieda, O. and Alzoubi, K.A. (2004), "Fracture mechanisms of offset rock joints-a laboratory investigation", *Geotech. Geol. Eng.*, **22**(4), 545-562.

Park, C.H. (2008), "Coalescence of frictional fractures in rock materials", Ph.D. Dissertation, Purdue University West Lafayette, Indiana, U.S.A.

Petit, J. and Barquins, M. (1988), "Can natural faults propagate under mode II conditions?", *Tecton.*, **7**(6), 1243-1256.

Potyondy, D.O. and Cundall, P.A. (2004), "A bonded-particle model for rock", *Int. J. Rock Mech. Min. Sci.*, **41**(8), 1329-1364.

Reyes, O. and Einstein, H.H. (1991), "Failure mechanism of fractured rock-a fracture coalescence model", *Proceedings of the 7th International Congress of Rock Mechanics*.

Sanchez, J. (1979), "Application of the disk test to mode-I-II fracture toughness analysis", M.Sc. Dissertation, University of Pittsburgh, Pittsburgh, U.S.A.

Sarfarazi, V., Ghazvinian, A., Schubert, W., Blumel, M. and Nejati, H.R. (2014), "Numerical simulation of the process of fracture of echelon rock joints, rock mechanics and rock engineering", **47**(4), 1355-1371.

Sarfarazi, V., Haeri, H. and Bagher Shemirani, A. (2017a), "Direct and indirect methods for determination of mode I fracture toughness using PFC2D", *Comput. Concrete*, **20**(1), 39-47.

Sarfarazi, V., Haeri, H., Bagher Shemirani, A. and Zhu, Z. (2017b), "The effect of compression load and rock bridge geometry on the shear mechanism of weak plane", *Geomech. Eng.*, **13**(3), 57-63.

Sarfarazi, V., Haeri, H., Bagher Shemirani, A., Hedayat, A. and Hosseini, S. (2017c), "Investigation of ratio of TBM disc spacing to penetration depth in rocks with different tensile strengths using PFC2D", *Comput. Concrete*, **20**(4), 429-437.

Scavia, C. and Castelli, M. (1998), "Studio della propagazione per trazione indotta di sistemi di fratture in roccia", *Rivista Italiana di Geotecnica*, anno XXXII, 48-62.

Shaowei, H., Aiqing, X., Xin, H. and Yangyang, Y. (2016), "Study on fracture characteristics of reinforced concrete wedge splitting tests", *Comput. Concrete*, **18**(3), 337-354.

Shemirani, A., Naghdabadi, R. and Ashrafi, M. (2016), "Experimental and numerical study on choosing proper pulse shapers for testing concrete specimens by split Hopkinson pressure bar apparatus", *Constr. Build. Mater.*, **125**, 326-336.

Shen, B. and Stephansson, O. (1993), "Large-scale permeability tensor of rocks from induced microseismicity", *Int. J. Rock

Mech. Min. Sci. Geomech. Abstr., **30**, 861-867.
Shen, B., Stephansson, O., Einstein, H.H. and Ghahreman, B. (1995), "Large-scale permeability tensor of rocks from induced micro-seismicity", *J. Geophys. Res.*, **100**, 5975-5990.
Shetty, D.K., Rosenfield, A.R. and Duckworth, W.H. (1986), "Mixed mode fracture of ceramic in diametrical compression", *J. Am. Ceram. Soc.*, **69**(6), 437-443.
Wang, Q.Z. (2010), "Formula for calculating the critical stress intensity factor in rock fracture toughness tests using cracked chevron notched Brazilian disc (CCNBD) specimens", *Int. J. Rock Mech. Min. Sci.*, **47**(6), 1006-1011.
Wang, Q.Z., Feng, F., Ni, M. and Gou, X.P. (2011), "Measurement of mode I and mode II rock dynamic fracture toughness with cracked straight through flattened Brazilian disc impacted by split Hopkinson pressure bar", *Eng. Fract. Mech.*, **78**(12), 2455-2469.
Wang, Q.Z., Gou, X.P. and Fan, H. (2012), "The minimum dimensionless stress intensity factor and its upper bound for CCNBD fracture toughness specimen analyzed with straight through crack assumption", *Eng. Fract. Mech.*, **82**, 1-8.
Wang, X., Zhu, Z., Wang, M., Ying, P., Zhou, L. and Dong, Y. (2017), "Study of rock dynamic fracture toughness by using VB-SCSC specimens under medium-low speed impacts", *Eng. Fract. Mech.*, **181**, 52-64.
Wei, M.D., Dai, F., Xu, N.W., Xu, Y. and Xia, K. (2015), "Three-dimensional numerical evaluation of the progressive fracture mechanism of cracked chevron notched semi-circular bend rock specimens", *Eng. Fract. Mech.*, **134**, 286-303.
Wong, R.H.C. and Chau, K.T. (1998), "Crack coalescence in a rock-like material containing two cracks", *Int. J. Rock Mech. Min. Sci.*, **35**(2), 147-164.
Wong, R.H.C., Tang, C.A., Chau, K.T. and Lin, P. (2002), "Splitting failure in brittle rocks containing pre-existing flaws under uniaxial compression", *Eng. Fract. Mech.*, **69**(1), 853-871.
Yang, S.Q. (2015), "An experimental study on fracture coalescence characteristics of brittle sandstone specimens combined various flaws", *Geomech. Eng.*, **8**(4), 541-557.

CC